Element-specific depth profile of magnetism and stoichiometry at the La0.67Sr0.33MnO3/BiFeO3 interface

PHYSICAL REVIEW B **90**, 041113(R) (2014)

Element-specific depth profile of magnetism and stoichiometry at the $La_{0.67}Sr_{0.33}MnO_3/BiFeO_3$ interface

J. Bertinshaw,[1,2] S. Brück,[1,2] D. Lott,[3] H. Fritzsche,[4] Y. Khaydukov,[5] O. Soltwedel,[5] T. Keller,[5] E. Goering,[6] P. Audehm,[6] D. L. Cortie,[2] W. D. Hutchison,[7] Q. M. Ramasse,[8] M. Arredondo,[9] R. Maran,[10] V. Nagarajan,[10] F. Klose,[2,11] and C. Ulrich[1,2]

[1]*School of Physics, University of New South Wales, Sydney, NSW 2052, Australia*
[2]*Australian Nuclear Science and Technology Organisation, Lucas Heights, NSW 2234, Australia*
[3]*Institute for Materials Research, Helmholtz Zentrum Geesthacht, D-21502 Geesthacht, Germany*
[4]*Canadian Neutron Beam Centre, Chalk River Laboratories, Ontario, Canada K0J 1J0*
[5]*Max-Planck-Institute for Solid State Research, outstation FRM II, D-70569 Stuttgart, Germany*
[6]*Max-Planck-Institute for Intelligent Systems, D-70569 Stuttgart, Germany*
[7]*School of Physical, Environmental and Mathematical Sciences, University of New South Wales, Canberra, ACT 2600, Australia*
[8]*SuperSTEM Laboratory, STFC Daresbury Campus, Keckwick Lane, Daresbury WA4 4AD, United Kingdom*
[9]*School of Mathematics and Physics, Queen's University Belfast, Belfast BT7 1NN, United Kingdom*
[10]*School of Materials Science and Engineering, University of New South Wales, Sydney, NSW 2052, Australia*
[11]*Department of Physics and Materials Science, City University of Hong Kong, Hong Kong SAR, China*

(Received 1 July 2013; revised manuscript received 11 July 2014; published 31 July 2014)

Depth-sensitive magnetic, structural, and chemical characterization is important in the understanding and optimization of physical phenomena emerging at the interfaces of transition metal oxide heterostructures. In a simultaneous approach we have used polarized neutron and resonant x-ray reflectometry to determine the magnetic profile across atomically sharp interfaces of ferromagnetic $La_{0.67}Sr_{0.33}MnO_3$/multiferroic $BiFeO_3$ bilayers with subnanometer resolution. In particular, the x-ray resonant magnetic reflectivity measurements at the Fe and Mn resonance edges allowed us to determine the element-specific depth profile of the ferromagnetic moments in both the $La_{0.67}Sr_{0.33}MnO_3$ and $BiFeO_3$ layers. Our measurements indicate a magnetically diluted interface layer within the $La_{0.67}Sr_{0.33}MnO_3$ layer, in contrast to previous observations on inversely deposited layers [P. Yu *et al.*, Phys. Rev. Lett. **105**, 027201 (2010)]. Additional resonant x-ray reflection measurements indicate a region of altered Mn and O content at the interface, with a thickness matching that of the magnetic diluted layer, as the origin of the reduction of the magnetic moment.

DOI: 10.1103/PhysRevB.90.041113 PACS number(s): 75.25.−j, 61.05.cm, 75.70.Cn, 77.55.Nv

Emergent electronic states in transition metal oxide (TMO) thin film multilayered structures have created significant attention recently [1–6]. Unexpected properties, not present in the respective bulk constituents, were demonstrated, such as metallic conductivity at the interface between two insulators, or even superconducting behavior [4]. Fundamentally, these states are a consequence of the symmetry breaking at the interface between dissimilar oxide materials [6]. The resulting interface-near electronic states are defined by spin exchange correlations, orbital reconstructions, band bending, Coulombic, magnetic, or superconducting penetration into the adjacent layer, and epitaxial strain across the interface [5–8]. As pointed out by Hwang *et al.* [6], their detailed origin is still under debate since standard experimental techniques do not allow for the separation of intrinsic interface effects from modifications in the chemical composition, in particular, oxygen deficiencies. This requires different experimental techniques, which, in particular, can determine the chemical depth profile across the interfaces with subnanometer resolution.

Two particularly interesting TMO materials are the multiferroic bismuth ferrite, $BiFeO_3$ (BFO), and the ferromagnetic (FM) half-metal $La_{0.67}Sr_{0.33}MnO_3$ (LSMO), which constitutes an almost completely spin-polarized electron system. While for bulk LSMO the surface depolarizes the spins [9], the problem can be largely overcome in TMO thin film structures. BFO in itself is an exciting multiferroic compound, since it exhibits spontaneous magnetic ($T_N = 643$ K) and electric ($T_C = 1143$ K) polarization well above room temperature [10]. Both order parameters are indirectly coupled, i.e., the spin state can be controlled through an electric field [11]. LSMO/BFO/LSMO trilayers exhibit a large tunnel magnetoresistance (TMR). Interestingly, voltage-induced changes in the TMR behavior were recently demonstrated in Refs. [12,13]. This opens possibilities for multilevel memory state applications for next-generation information storage devices [14]. It is unclear, however, if the observed TMR effect is at its optimum. Any magnetic interface modification leading to a perturbation of the spin-polarized flow at the LSMO interface would decrease the efficiency of such a device [3]. Therefore, it is imperative to precisely identify the chemical and magnetic properties of the interface states.

In this Rapid Communication we demonstrate the influence of changes in the chemical composition on the interface magnetism of LSMO/BFO bilayers. The combination of complementary x-ray and neutron techniques provided insight into the magnetic and chemical depth profile of the bilayer interface. The simultaneous analysis of polarized neutron reflectivity (PNR) and element-specific x-ray resonant magnetic reflectometry (XRMR) provided a means of accurately determining the magnetic properties with subnanometer resolution across the interface. Element-specific resonant soft x-ray reflectivity (XRR) and XRMR measurements performed at the Fe $L_{2,3}$ and Mn $L_{2,3}$ edges allowed for the determination of the magnetic moments in the individual layers and indicated an altered stoichiometry at the interface as the reason for an observed reduction of the magnetic moment.

LSMO (300 Å)/BFO (200 and 300 Å) bilayers were grown epitaxially on a $SrTiO_3$ (STO) (001) substrate using a Neocera pulsed laser deposition (PLD) system with a 248 nm wavelength KrF excimer laser. The atomic precision of the layer-by-layer growth was calibrated by reflection high electron energy diffraction (RHEED). Oxygen partial pressures of 100/10 mTorr and substrate temperatures of 900/850 °C were held for the deposition of the LSMO/BFO layers, respectively. The deposited bilayer was cooled in a partial oxygen pressure of 200 Torr at a rate of 20 K/min (for further details, see Ref. [13]). The bilayers were initially characterized by laboratory x-ray diffraction and x-ray reflection (instrument X'Pert Pro), which reveal an epitaxial growth with a root-mean-squared (rms) interface roughness of 5(1) Å. This result is consistent with scanning transmission electron microscopy (STEM) images on samples grown under identical conditions, which show a sharp coherent interface (see the Supplemental Material [15]). These results demonstrate the excellent quality of our films, and rules out interdiffusion larger than 5 Å across the interface. To compensate for in-plane stress caused by the lattice mismatch, the c-axis lattice parameter was elongated in the 200 Å thick BFO layer from 3.965 to 4.081(5) Å, i.e., by 3.0%, and compressed for LSMO from 3.871 to 3.8505 Å, i.e., −0.55%. This indicates a partial back-relaxation from the expected change in the c-axis lattice parameter, as observed in Ref. [16].

Magnetization measurements performed using the Quantum Design physical property measurement system (PPMS) and magnetic property measurement system (MPMS) revealed that the LSMO layer orders ferromagnetically below $T_C = 345(5)$ K (see the Supplemental Material [15]). This corresponds to a reduction of the expected bulk value of 370 K [17]. In-plane hysteresis curves collected at $T = 150$ K showed a low coercivity of ∼1.7 mT and a saturated magnetic moment of $3.0\mu_B$/Mn ion, which is also smaller than the bulk values of $3.5\mu_B$/Mn ion [17]. This is in accordance with previous experiments [16,18,19] and is primarily caused by the in-plane epitaxial strain. The change in the c-axis lattice parameter, i.e., a modified c/a ratio, results in a biaxial tilt and deformation of the MnO_6 octahedra, which affects the orbital arrangement. This weakens the in-plane hopping integral and reduces the ferromagnetic double-exchange interaction. No further effects, such as modified Mn or O content in the bulk of the LSMO layer, are required to be accounted for, demonstrating the excellent quality of the films.

Polarized neutron reflectometry (PNR) is a powerful technique for the investigation of magnetic thin film systems [20]. An accurate depth profile of the absolute ferromagnetic moment can be determined through changes in the specular reflectance between spin-polarized neutron beams [21]. Reflectivity curves were measured using the instruments NREX, located at FRM-II, Munich, Germany, D3 at NRU, Chalk River, Canada, and on Platypus at ANSTO, Australia. Figure 1 shows characteristic reflectivity data taken with a Q_z resolution of ∼4%. The spin-up (R^{++}) and spin-down (R^{--}) neutron spin channels were measured to investigate the magnetic moment of the bilayer sample aligned parallel to an external applied field. Additional scans of the spin-flip channels R^{+-} and R^{-+}, which probe the magnetic moment perpendicular to the neutron polarization, showed no measurable signal,

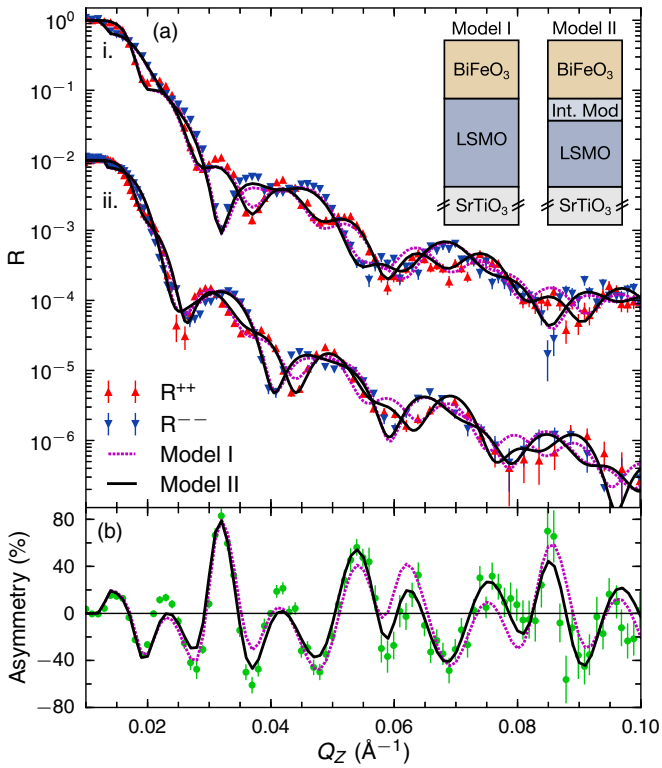

FIG. 1. (Color online) (a) Specular PNR reflectivity for the R^{++} and R^{--} channels of a (i) 300 Å LSMO/200 Å BFO sample taken at $T = 150$ K on the instrument NREX and (ii) of a 300 Å LSMO/300 Å BFO sample taken at $T = 300$ K on the instrument Platypus (the data are shifted in intensity). (b) Asymmetry between both channels of experiment (i). The dashed lines depict the less accurate two-layer simulation without any interfacial layers (model I). The solid lines correspond to the fit of the final model (model II), which is characterized by a 26 Å interface layer with a 40% suppressed magnetic moment.

indicating that the LSMO magnetization was fully aligned within the plane of the film. Figure 1(a) shows the R^{++} and R^{--} spin-dependent specular reflectivities of two different bilayer samples measured at (i) 150 K and (ii) 300 K. The spin asymmetry ($A = \frac{R^{++}-R^{--}}{R^{++}+R^{--}}$) for the 150 K data is plotted in Fig. 1(b). The temperature of 150 K was chosen since it is well below T_C of the LSMO layer and above a structural phase transition of the STO substrate at 110 K [22]. To ensure full saturation of the Mn-ion moments, the sample was field cooled under an applied magnetic field of 0.5 T parallel to the neutron polarization. Measurements were performed with an external magnetic field of 0.7 mT, required to maintain the polarization of the neutron beam. In this way, the effect of an external magnetic field on the interface was minimized while maximizing the contrast between spin channels. The SIMULREFLEC software package was used to perform a simultaneous least squares fit [23]. Specific parameters already determined by XRR, i.e., layer thicknesses, density, and nonmagnetic interface roughness, were fixed during the fitting process. The dashed lines in Fig. 1 correspond to the fitting of a two-layer system of LSMO and BFO without an interfacial layer (model I). A significant improvement to the fit, with a reduction of the residual error

from 6.094 to 3.147 (see the Supplemental Material [15]), was obtained when including an additional magnetically diluted interface layer of 26(5) Å with a 40% suppressed magnetic moment of $1.8(2)\mu_B$/Mn ion instead of the $2.6(3)\mu_B$/Mn ion of the bulk of the LSMO layer (model II). Additional magnetic layers at the STO/LSMO interface or at the BFO/air interface did not yield any convincing improvement of the fit.

In order to firmly determine whether the ferromagnetic diluted interface layer is located within the LSMO, the BFO, or across the interface, we have performed element-specific x-ray resonant magnetic reflection (XRMR) measurements at the Fe L_3 and Mn L_3 edges. XRMR is an extension of standard reflectometry with the use of x-ray magnetic circular dichroism (XMCD) [24]. Measurements were performed at the UE56/2-PGM1 beamline at the BESSY II synchrotron of the Helmholtz Center Berlin, Germany at the ERNSt endstation of the Max Planck Institute for Intelligent Systems, Stuttgart, Germany [24]. A representative Fe $L_{2,3}$ x-ray absorption spectrum (XAS) of the sample in total electron yield (TEY) is shown in Fig. 2, together with XRMR curves taken at the Fe L_3 edge ($E = 708.4$ eV) for parallel and antiparallel alignment of the magnetization vector of the sample and the x-ray beam polarization vector. The XRMR curves in Figs. 2(b) and 2(c) show that the measurements taken for both polarizations are quasi-identical. This already indicates the absence of any sizable ferromagnetic moment in the BFO layer. Figure 3(a) shows the magnetic asymmetry ratio of the Q_z measurement taken at the Fe L_3 edge [from the data of Fig. 2(b)]. Simulations of hypothetical FM signals in BFO are shown for comparison (program REMAGX [25]). A magnetic polarization of $0.2\mu_B/Fe^{3+}$ in the first 10 Å (gray area) and 20 Å (yellow area) of BFO at the LSMO interface was assumed. Using literature data for the magneto-optical constants [26] and for the scaling [27], the simulations clearly show that even such a small moment would result in a sizable magnetic asymmetry. Our measurements do not show any ferromagnetic signal originating from the Fe ions in the BFO layer down to a noise level of 0.3%, indicating that the Fe magnetic moments are not larger than $0.04\mu_B/Fe^{3+}$ in the BFO layer.

As the next step, measurements were performed at the Mn L_3 edge at $E = 643.1$ eV [see Fig. 3(b)]. Qualitative XAS was measured via fluorescence emission and used to calibrate literature reference data for LSMO [28–30] to obtain the optical and magneto-optical index of refraction for LSMO. The degree of circular polarization of 90% for the present measurements was taken into account when calculating the magneto-optical part of the index of refraction. Figure 3(b)

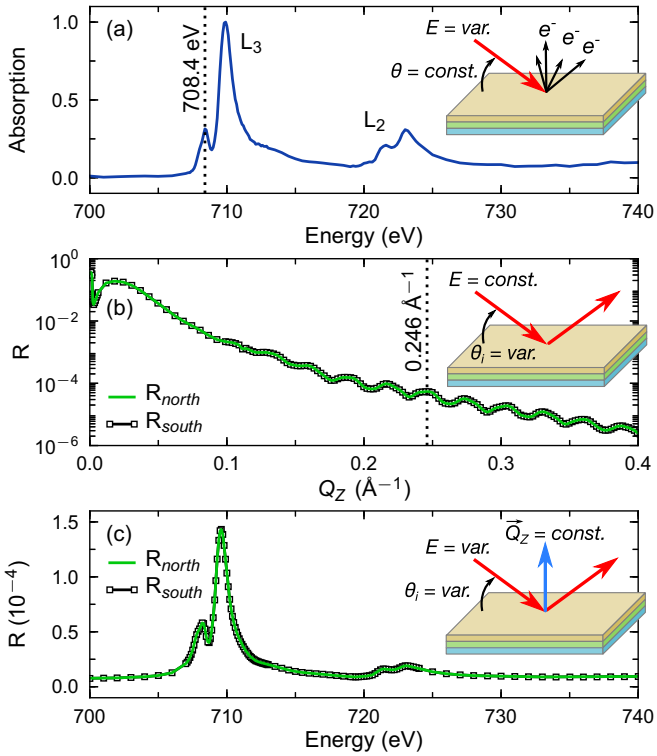

FIG. 2. (Color online) (a) XAS in the vicinity of the Fe $L_{2,3}$edges for unpolarized x rays. (b) XRMR curves (parallel and antiparallel) measured at an energy of $E = 708.4$ eV using positive circular polarized x rays and a flipped external magnetic field of 80 mT. No visual difference between the two curves is apparent, implying the absence of a sizable magnetic signal. (c) Reflected intensity energy scan at $Q_z = 0.246$ Å^{-1}, a point of the reflectivity curve that would show a significant splitting in the presence of FM contribution.

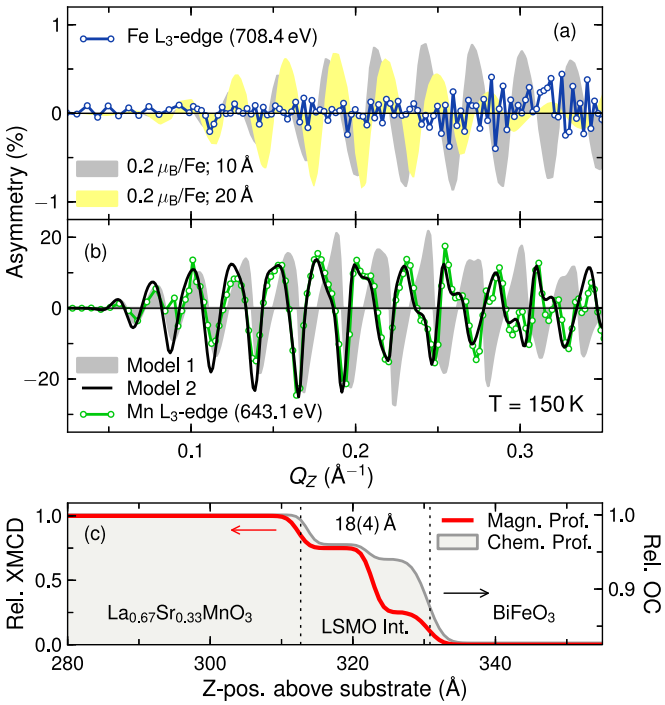

FIG. 3. (Color online) (a) XRMR magnetic asymmetry signal at the Fe L_3 edge at 708.4 eV conclusively indicates no Fe ferromagnetic signal. The shaded areas show simulated asymmetries for a hypothetical magnetic moment of $0.2\mu_B$/Fe in the first 10 Å (gray area) and 20 Å (yellow area). (b) XRMR magnetic asymmetry measured at the Mn L_3 edge at 643.1 eV. The best agreement is obtained for a model with a LSMO interfacial layer with reduced magnetization (black line). For comparison, a homogenous magnetized LSMO layer does not reproduce the periodicity for smaller Q_z (gray area). (c) Resulting magnetic depth profile. The relative optical constant obtained from resonant XRR, which indicates the change in the chemical profile, is shown as well.

shows a significant magnetic asymmetry for the Mn L_3 edge, indicating a spontaneous FM polarization. By simulating the Mn magnetic asymmetry we derived the Mn-specific magnetic depth profile. The magnetic reflectivity calculations were based on a magneto-optical approach to fit to the measured reflectivity data [31], where the polarization dependence of the incident x-ray beam upon the direction of the dielectric susceptibility tensor is taken into account. We again applied model I (see Fig. 1) without an interfacial layer between the LSMO and BFO layers (gray area). In this case the oscillations of the asymmetry signal cannot be reproduced. The best fit to the data is obtained when an interface layer with a gradually reduced magnetic moment in the top 18(4) Å of the LSMO layer was introduced [see the solid line in Fig. 3(b)]. The resulting magnetic profile is shown in Fig. 3(c). This is in good agreement with the result obtained by PNR. The combined PNR and XRMR analysis indicates a depleted FM region extending about 20 Å into the LSMO at the bilayer interface.

Our results are in contrast to previous XMCD measurements on an inverse BFO/LSMO bilayer, which yielded an induced FM interface layer with a magnetic moment of $0.6\mu_B/Fe^{3+}$ ion within the BFO [1]. A similar result was obtained on a 180 Å BFO layer with a top layer of 75 Å of CoFeB [20]. PNR measurements on this bilayer indicated a 20 Å interfacial layer with a FM moment of $1\mu_B/Fe^{3+}$ extending into the BFO layer. The induced FM magnetic moment was explained by orbital or spin reconstructions at the interface.

In order to elucidate the origin of the reduction of the magnetic moment at the LSMO/BFO interface, we have performed intrinsic element-specific resonant x-ray reflectivity measurements with linear polarization at the ERNSt endstation at BESSY-II. This did yield valuable information on the local chemistry and valences at the LSMO/BFO interface. Using the results of the XAS study (data not shown here), XRR curves were collected at $T = 150$ K for the Mn L_3 edge at the maximum of the XAS signal at 644.1 eV and of resonance at 900 eV. Similarly to the XRMR analysis, simulations of the XRR experimental data were performed with an algorithm we developed. The XRR curves and the fitted results are shown in Fig. 4. It is important to note that our experiments indicate that the bulk of the LSMO and BFO layers exhibit ideal stoichiometry, and that rms interfacial roughnesses between the $SrTiO_3$ substrate, LSMO, and BFO were found to be no larger than 5(1) Å. The simulations did indicate that the XRR data collected in an off-resonance condition are highly sensitive to modifications within the BFO layer. A significant improvement of the theoretical fit to the data was achieved by including a 18(5) Å thick top layer with a 10% changed optical constant (black line versus dotted line). This indicates a modification of the BFO stoichiometry towards impurity phases at the BFO interface to air.

Resonant XRR measurements performed at the Mn L_3 edge offer the opportunity to detect small alterations in the depth profile of the Mn stoichiometry. The analysis of the Mn XRR data indicated a 17(5) Å layer inside the LSMO layer at the interface between LSMO and BFO with a variation of the optical constants (OCs) of about 5% (see the black solid line in Fig. 4 in contrast to the purple dotted line for the simpler model assuming homogeneous layers). As the

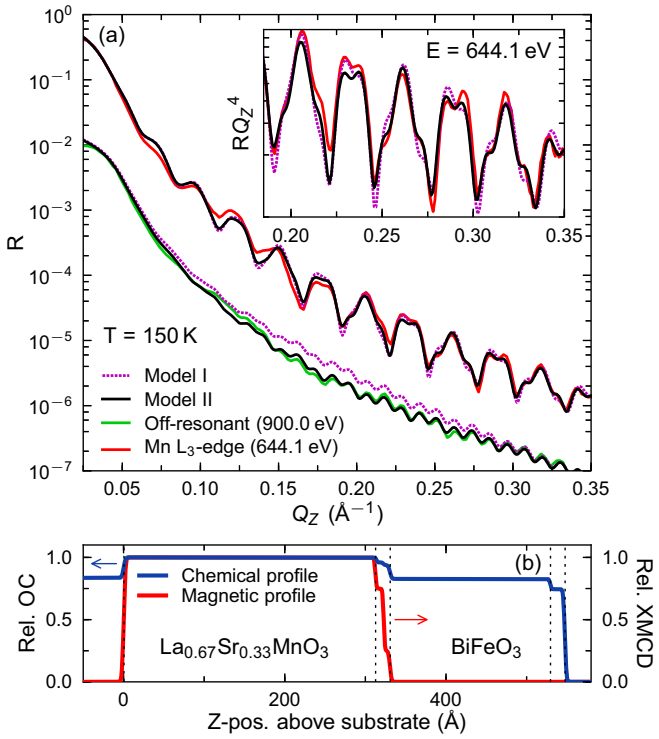

FIG. 4. (Color online) (a) X-ray reflectivity data measured at 644.1 and 900.0 eV, i.e., resonant at the Mn L_3 edge and off resonant. The data was fitted using two different models as described in the text. The inset shows RQ_z^4 in the most sensitive high Q_z region. (b) Resulting chemical (through XRR) and magnetic (PNR and XRMR) depth profiles.

optical properties vary strongly close to the resonance peak of the Mn L_3 edge, the absolute change in stoichiometry cannot be precisely quantified. However, the data points towards a modification of the interface stoichiometry with an altered oxygen and Mn content in this region [28,32,33]. Even a slight modification in the oxygen and Mn concentration would result in a significant deviation of the Mn^{3+}/Mn^{4+} ratio. This would have a direct impact on the concentration of the charge carriers which mediate the double-exchange interaction between the ferromagnetically coupled ions. As a consequence, the magnetic phase transition temperature and the ordered magnetic moment decrease [17]. Indeed, an extrapolation of the temperature dependent PNR data indicates that the interfacial layer has a reduced T_C of 316(10) K (see the Supplemental Material [15]). The thickness of this chemically altered interfacial layer matches exactly with the region of the reduced magnetic moment as determined independently by PNR and XRMR. This reduction over five to six octahedral sites cannot be explained by epitaxial strain effects alone. Spin and orbital reconstruction right at the interface will also not fully account for this effect since both would only take place in the topmost atomic layer. This indicates that the modified magnetic properties in the interface region between the LSMO and BFO layers are mainly caused by an altered oxygen and Mn concentration.

In conclusion, we have demonstrated that a combination of complementary reflectometry techniques allowed for the precise determination of the magnetic and chemical depth

profiles in LSMO/BFO heterostructures. Resonant element-specific x-ray reflection measurements indicated an interface region of modified oxygen or Mn content with the same thickness as the magnetically diluted interfacial layer within the LSMO film, as determined by the magnetic XRMR and PNR measurements. This magnetically diluted layer hinders the spin-polarized current across the interface and hence deteriorates the functionality of tunneling junctions. Therefore, our result underlines the importance of the precise knowledge of the chemical composition at the interface. Modifications in the stoichiometry can occur during the growth interruption, when the LSMO and the BFO layers were completed [20]. This is a common problem for all transition metal oxide thin film systems. Previous investigations have shown that the atomic concentrations at the interface can be controlled systematically by the growth process [2,16,18]. Changing the deposition conditions would allow for the engineering of the interface structure and thus enable the growth of artificial heterostructures with specifically desired properties.

The authors would like to thank D. Manske at the MPI-FKF, Stuttgart, Germany, for fruitful discussions and careful reading of the manuscript. This work was supported by the Australian Research Council through Grant No. DP110105346 and by AINSE. V.N. and R.M. acknowledge the support of the ARC (Grant No. LP0991794). Electron microscopy was carried out at the National Center for Electron Microscopy, Lawrence Berkeley National Laboratory, supported by the US Department of Energy under Contract No. DE-AC02-05CH11231.

[1] P. Yu, J.-S. Lee, S. Okamoto, M. D. Rossell, M. Huijben, C.-H. Yang, Q. He, J. X. Zhang, S. Y. Yang, M. J. Lee, Q. M. Ramasse, R. Erni, Y.-H. Chu, D. A. Arena, C.-C. Kao, L. W. Martin, and R. Ramesh, Phys. Rev. Lett. **105**, 027201 (2010).

[2] A. Ohtomo and H. Y. Hwang, Nature (London) **427**, 423 (2004).

[3] H. Yamada, Y. Ogawa, Y. Ishii, H. Sato, M. Kawasaki, H. Akoh, and Y. Tokura, Science **305**, 646 (2004).

[4] N. Reyren, S. Thiel, A. D. Caviglia, L. Fitting Kourkoutis, G. Hammerl, C. Richter, C. W. Schneider, T. Kopp, A.-S. Rüetschi, D. Jaccard, M. Gabay, D. A. Müller, J.-M. Triscone, and J. Mannhart, Science **317**, 1196 (2007).

[5] J. Mannhart and D. G. Schlom, Science **327**, 1607 (2010).

[6] H. Y. Hwang, Y. Iwasa, M. Kawasaki, B. Keimer, N. Nagaosa, and Y. Tokura, Nat. Mater. **11**, 103 (2012).

[7] J. Chakhalian, J. W. Freeland, H.-U. Habermeier, G. Cristiani, G. Khaliullin, M. van Veenendaal, and B. Keimer, Science **318**, 1114 (2007).

[8] N. Driza, S. Blanco-Canosa, M. Bakr, S. Soltan, M. Khalid, L. Mustafa, K. Kawashima, G. Christiani, H.-U. Habermeier, G. Khaliullin, C. Ulrich, M. Le Tacon, and B. Keimer, Nat. Mater. **11**, 675 (2012).

[9] M. Konoto, T. Kohashi, K. Koike, T. Arima, Y. Kaneko, Y. Tomioka, and Y. Tokura, Appl. Phys. Lett. **84**, 2361 (2004).

[10] G. Catalan and J. F. Scott, Adv. Mater. **21**, 2463 (2009).

[11] T. Zhao, A. Scholl, F. Zavaliche, K. Lee, M. Barry, A. Doran, M. P. Cruz, Y. H. Chu, C. Ederer, N. A. Spaldin, R. R. Das, D. M. Kim, S. H. Baek, C. B. Eom, and R. Ramesh, Nat. Mater. **5**, 823 (2006).

[12] H. Béa, M. Gajek, M. Bibes, and A. Bartélémy, J. Phys.: Condens. Matter **20**, 434221 (2008).

[13] M. Hambe, A. Petraru, N. A. Pertsev, P. Munroe, V. Nagarajan, and H. Kohlstedt, Adv. Funct. Mater. **20**, 2436 (2010).

[14] W. Eerenstein, N. D. Mathur, and J. F. Scott, Nature (London) **442**, 759 (2006).

[15] See Supplemental Material at http://link.aps.org/supplemental/10.1103/PhysRevB.90.041113 for complementary STEM and EELS data, and additional information on the magnetometry and reflectometry studies.

[16] M. Angeloni, G. Balestrino, N. G. Boggio, P. G. Medaglia, P. Orgiani, and A. Tebano, J. Appl. Phys. **96**, 6387 (2004).

[17] A. Urushibara, Y. Moritomo, T. Arima, A. Asamitsu, G. Kido, and Y. Tokura, Phys. Rev. B **51**, 14103 (1995).

[18] P. Lecoeur, A. Gupta, P. R. Duncombe, G. Q. Gong, and G. Xiao, J. Appl. Phys. **80**, 513 (1996).

[19] Y. Konishi, Z. Fang, M. Izumi, T. Manako, M. Kasai, H. Kuwahara, M. Kawasaki, K. Terakura, and Y. Tokura, J. Phys. Soc. Jpn. **68**, 3790 (1999).

[20] H. Béa, M. Bibes, F. Ott, B. Dupé, X.-H. Zhu, S. Petit, S. Fusil, C. Deranlot, K. Bouzehouane, and A. Barthélémy, Phys. Rev. Lett. **100**, 017204 (2008).

[21] M. R. Fitzsimmons, S. D. Bader, J. A. Borchers, G. P. Felcher, J. K. Furdyna, A. Hoffmann, J. B. Kortright, I. K. Schuller, T. C. Schulthess, S. K. Sinha, M. F. Toney, D. Weller, and S. Wolf, J. Magn. Magn. Mater. **271**, 103 (2004).

[22] G. Shirane and Y. Yamada, Phys. Rev. **177**, 858 (1969).

[23] "SIMULREFLEC—Reflectivity Curves Simulations and Fitting," Institute Laue Langevin, 2010.

[24] S. Brück, S. Bauknecht, B. Ludescher, E. Goering, and G. Schütz, Rev. Sci. Instrum. **79**, 083109 (2008).

[25] S. Macke, S. Brück, and E. Goering, "REMAGX—x-ray magnetic reflectivity tool," 2010.

[26] H. Béa, M. Bibes, S. Fusil, K. Bouzehouane, E. Jacquet, K. Rode, P. Bencok, and A. Barthélémy, Phys. Rev. B **74**, 020101(R) (2006).

[27] L. W. Martin, Y.-H. Chu, M. B. Holcomb, M. Huijben, P. Yu, S.-J. Han, D. Lee, S. X. Wang, and R. Ramesh, Nano Lett. **8**, 2050 (2008).

[28] E. Pellegrin, L. H. Tjeng, F. M. F. de Groot, R. Hesper, G. A. Sawatzky, Y. Moritomo, and Y. Tokura, J. Electron. Spectrosc. Relat. Phenom. **86**, 115 (1997).

[29] J. W. Freeland, J. J. Kavich, K. E. Gray, L. Ozyuzer, H. Zheng, J. F. Mitchell, M. P. Warusawithana, P. Ryan, X. Zhai, R. H. Kodama, and J. N. Eckstein, J. Phys.: Condens. Matter **19**, 315210 (2007).

[30] S. Brück, S. Treiber, S. Macke, P. Audehm, G. Christiani, S. Soltan, H.-U. Habermeier, E. Goering, and J. Albrecht, New J. Phys. **13**, 033023 (2011).

[31] J. Zak, E. R. Moog, C. Liu, and S. D. Bader, Phys. Rev. B **43**, 6423 (1991).

[32] K. Horiba, A. Chikamatsu, H. Kumigashira, M. Oshima, N. Nakagawa, M. Lippmaa, K. Ono, M. Kawasaki, and H. Koinuma, Phys. Rev. B **71**, 155420 (2005).

[33] S. Picozzi, C. Ma, Z. Yang, R. Bertacco, M. Cantoni, A. Cattoni, D. Petti, S. Brivio, and F. Ciccacci, Phys. Rev. B **75**, 094418 (2007).